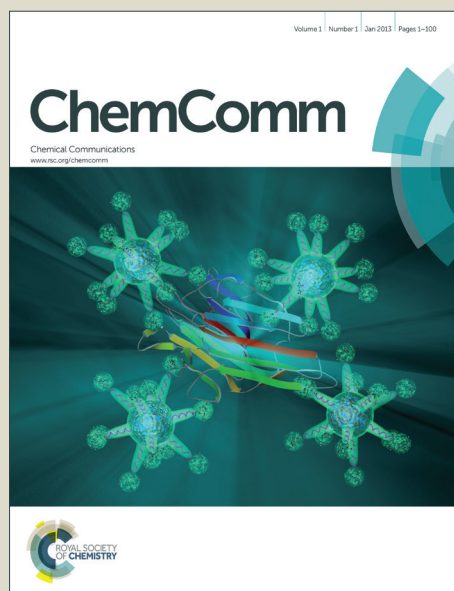


ChemComm

Accepted Manuscript



This is an *Accepted Manuscript*, which has been through the Royal Society of Chemistry peer review process and has been accepted for publication.

Accepted Manuscripts are published online shortly after acceptance, before technical editing, formatting and proof reading. Using this free service, authors can make their results available to the community, in citable form, before we publish the edited article. We will replace this *Accepted Manuscript* with the edited and formatted *Advance Article* as soon as it is available.

You can find more information about *Accepted Manuscripts* in the [Information for Authors](#).

Please note that technical editing may introduce minor changes to the text and/or graphics, which may alter content. The journal's standard [Terms & Conditions](#) and the [Ethical guidelines](#) still apply. In no event shall the Royal Society of Chemistry be held responsible for any errors or omissions in this *Accepted Manuscript* or any consequences arising from the use of any information it contains.

Solvent-induced reversible solid-state colour change of an intramolecular charge-transfer complex

Received 00th January 20xx,
Accepted 00th January 20xx

Ping Li,^a Josef M. Maier,^a Jungwun Hwang,^a Mark D. Smith,^a Jeanette A. Krause,^b Brian T. Mullis,^a Sharon M. S. Strickland,^c and Ken D. Shimizu^{a*}

DOI: 10.1039/x0xx00000x

www.rsc.org/

A dynamic intramolecular charge-transfer (CT) complex was designed that displayed reversible colour changes in the solid-state when treated with different organic solvents. The origins of the dichromatism were shown to be due to solvent-inclusion, which induced changes in the relative orientations of the donor pyrene and acceptor naphthalenediimide units.

Aromatic CT complexes¹ have found applications in host-guest complexes,^{2,3} supramolecular assemblies,^{4,5,6} self-healing^{7,8,9} and responsive materials,^{10,11,12} and organic electronics.^{13,14} Interestingly, aromatic CT interactions have not been as widely utilized in sensing applications, which is probably due to their low extinction coefficients and/or low association constants.^{15,16,17} However, CT interactions have a number of unique characteristics that are advantageous for sensing, molecular switches, and dynamic supramolecular systems. First, CT complexes typically absorb in the visible region of the UV-vis spectrum, and thus CT sensors can be monitored by the naked-eye. Second, the colours of CT complexes are highly sensitive to the electronic properties of the donor and acceptor units¹⁸ and to the relative geometry of the donor and acceptor units.^{19,20,21} Thus, binding effects that induce changes in the CT complex geometry can be easily monitored by variations in their colours.^{15,16,17,22,23}

The goal of this study was to develop a responsive colorimetric system based on an intramolecular CT interaction. Unlike the majority of CT sensors,²⁴ CT molecule **1** contains both the donor and acceptor units. The two pyrene (PYR) donor units are linked to a central 1,4,5,8-naphthalenediimide (NDI) acceptor unit (Fig 1a) forming a sandwich-type 2:1 aromatic stacking complex. Thus, the guest molecule does

not need to contain a donor or acceptor unit, which greatly expands the number of potential guests and the general utility of this design. The sensing mechanism is the guest-induced changes in geometry of the intramolecular CT interaction, which could be monitored by changes in colour of the CT complex.

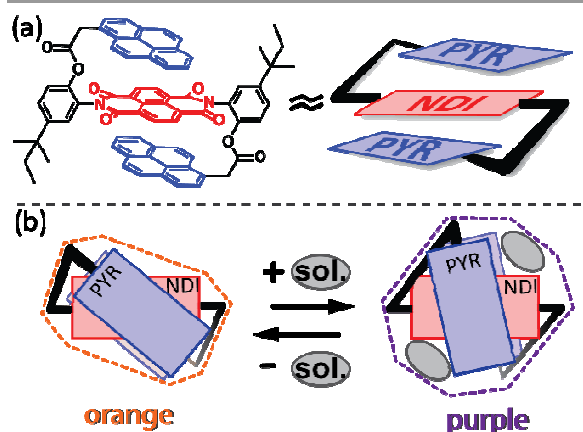


Fig. 1 (a) Molecular CT platform **1** highlighting the intramolecular donor-acceptor sandwich complex; and (b) a schematic representation of the solvation-desolvation induced complexation change in colour and geometry in **1**

The CT molecule **1** was readily prepared in three steps from commercially available 1-pyreneacetic acid, 2-amino-4-*tert*-amylphenol, and 1,4,5,8-naphthalenedianhydride (Scheme 1).²⁵ The two PYR donor units were connected to the central NDI acceptor unit via two short but flexible linkers, which ensured the formation of the intramolecular aromatic stacking complex but also allowed sufficient conformational freedom to allow the donor and acceptor units to adopt different geometries. The 5-atom linker (-C=C-O-C-C) was designed based on a similar 5-atom linker that was previously used to form a similar sandwich aromatic stacking complex around a NDI core.²⁶ Since **1** did not contain recognition groups that form strong directional interactions, the guest-induced colorimetric properties of **1** were initially studied in the solid-state where the confined condensed-phase environment could

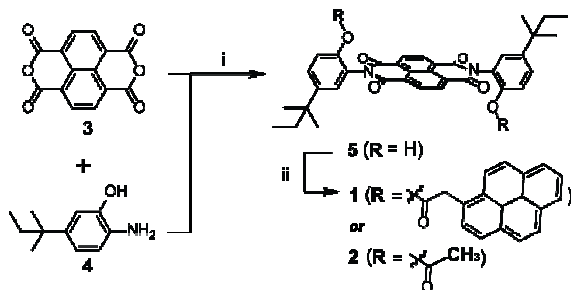
^a Department of Chemistry and Biochemistry, University of South Carolina, Columbia, SC 29208, United States.

^b Department of Chemistry, University of Cincinnati, Cincinnati, OH 45221, United States.

^c Department of Biology, Chemistry, and Physics, Converse College, Spartanburg, SC 29302, United States.

† Electronic Supplementary Information (ESI) available: Additional figures and tables, details of experimental, X-ray characterization, and NMR spectra. CCDC 1412209-1412215 For ESI and crystallographic data in CIF see DOI: 10.1039/x0xx00000x

allow guest molecules to sterically influence the relative geometry of the donor and acceptor units. Thus, the 2:1 PYR to NDI stoichiometry of the sandwich complex^{26, 27} was important to ensure that both surfaces of the NDI would be occupied and could not form additional interactions with adjacent molecules of **1**.²⁸



Scheme 1. Synthesis of the molecular CT model **1** and control **2**.

The ability of **1** to form an intramolecular CT complex was first confirmed in solution by the observation of the distinctive CT band in the visible region of the absorption spectrum. The λ_{max} at 505 nm was consistent with previous reports of PYR-NDI CT complexes.^{3,6,9,11,29,30,31} The effectiveness of the linker in forming and maintaining the intramolecular PYR-NDI complexation was also demonstrated by comparison with an intermolecular PYR-NDI complex formed between pyrene and control **2**, a structural analogue containing the same symmetrically substituted NDI core but lacking of the two pyrene donor groups. The intermolecular **2**•pyrene complex displayed a similar CT band (λ_{max} at 510 nm) but only at higher concentrations (> 10 mM).

Next, the observation of different coloured solid samples of **1** upon treatment with different solvents provided the first indications that the geometry and colour of the intramolecular CT complex in **1** were sensitive to solvent inclusion. When **1** was precipitated from dichloromethane, a purple solid was obtained, which was similar to the colour of **1** in solution. However, when **1** was precipitated from acetone, a distinctly different orange coloured solid was obtained. The purple and orange solids of **1** were further characterized by diffuse reflectance UV-vis spectroscopy (Fig 2). The purple solid of **1** showed a well-resolved CT absorption band with a λ_{max} at 530 nm. In comparison, the orange solid of **1** showed a similar but blue-shifted CT band with a λ_{max} at 500 nm. By comparison, control **2**, which only contained an NDI unit showed no CT band in the visible region of the diffuse reflectance UV-vis spectrum.

¹H NMR and HRMS analysis confirmed that both the purple and orange solids contained pure samples of **1**. The only differences were that the purple solid was a solvate of **1** containing two equivalents of dichloromethane; whereas, the orange solid was a non-solvate of **1**. Thermogravimetric analysis (TGA) of the purple solid further confirmed the presence of two CH₂Cl₂ molecules. A clear weight loss of

13% was observed when the purple solid was heated to 180 °C, which was consistent with the loss of two equivalents of CH₂Cl₂. After heating in the TGA, the purple solid became red-orange.³² In contrast, the orange solid showed no observable weight loss on heating in the TGA to 200 °C. Interestingly, the purple CH₂Cl₂-solvate of **1** was stable as the stoichiometry and coloration did not change after a month at room temperature as monitored by ¹H NMR and UV-vis spectrometry.

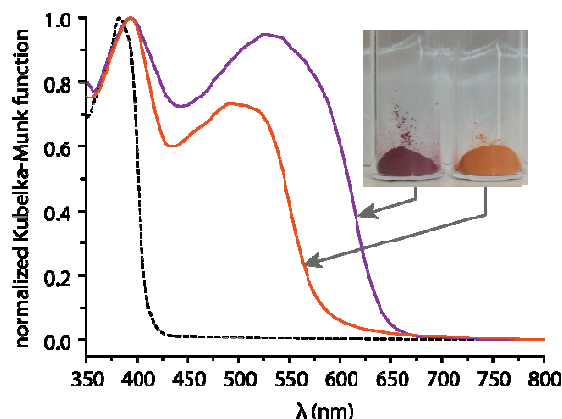


Fig 2. Normalized diffuse reflectance UV-vis spectra of the purple CH₂Cl₂-solvate solid of **1** (purple line), the orange non-solvate solid of **1** (orange line), and the white solid of control **2** (dotted black line).

The purple and orange solids of **1** could be easily and repeatedly interconverted by precipitation from the appropriate solvent. First, the purple CH₂Cl₂-solvate could be readily regenerated from the orange non-solvate by precipitation from dichloromethane (Fig 3a). Conversely, the orange non-solvate solid of **1** could be regenerated from purple **1** by precipitation from acetone. Acetone is a poor solvent for **1** and efficiently extracts any included solvent from solid samples of **1**. The ease with which **1** can uptake or lose included solvent molecules was demonstrated by simply wetting samples of **1** with a minimum amount of the CH₂Cl₂ or acetone, which yielded the corresponding colour change for the CH₂Cl₂ solvate or non-solvate forms, respectively (Fig S5).³³

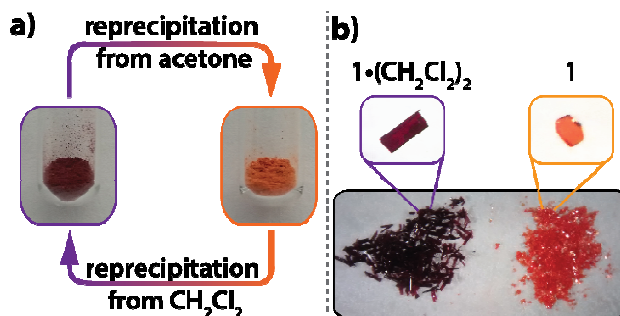


Fig. 3 (a) The reversible colour switching of solid **1** between purple CH₂Cl₂-solvate and orange non-solvate solid forms by precipitation from dichloromethane and acetone, respectively. (b) The CH₂Cl₂-solvate (left) and non-solvate (right) crystals of **1**, highlighting the distinct difference in colour.

To test the hypothesis that the different coloured solid forms of **1** were due to variations in the orientation of the PYR donor and NDI acceptor units in the intramolecular CT complex, X-ray quality single crystals of **1** from CH_2Cl_2 and acetone were obtained and analysed by X-ray crystallography (Fig 3b). Dark purple plate crystals were obtained from CH_2Cl_2 containing two equivalents of CH_2Cl_2 per **1** molecule. Conversely, orange thin plate crystals were obtained from acetone, which do not contain any trapped solvent molecules.³⁴ The colours of the crystals formed from each solvent were similar to the purple and orange solids formed in the earlier precipitation studies in the same two solvents. This suggested that the single crystals were the same structural forms as the coloured precipitated solids, which was confirmed in the matching XRD patterns for the precipitated solids with the simulated XRD patterns from the X-ray crystal structures (Fig S6).

Despite the differences in colour and solvation, the structures of the sandwich CT complexes in the purple and orange crystals of **1** were surprisingly similar (Fig 4). The folded conformations of **1** in both structures adopted the desired sandwich complex with the PYR donor units forming centrosymmetric aromatic stacking interactions on both faces of the central NDI unit (Fig 4). The PYR-center to NDI-plane distances (3.5 and 3.6 Å) for the solvate and non-solvate structures were very similar and were consistent with an intramolecular aromatic stacking interaction.

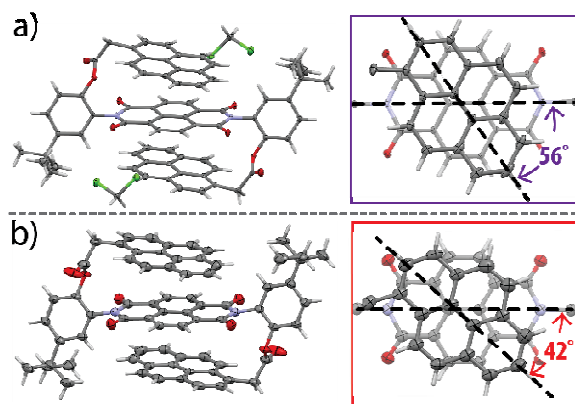


Fig 4. Side views of the X-ray structures of (a) the dark purple **1**•(CH_2Cl_2)₂ and (b) the orange non-solvate **1** crystals. Insets are top views of the PYR and NDI surfaces (with linkers, frameworks, and bottom PYR surface omitted for viewing clarity). The pyrene surfaces in both crystals were disordered and only the major conformers (76% and 72%) are shown.

To help identify the geometric variations that lead to the dramatic differences in colour of the solids, additional four crystal structures of **1** containing different solvent molecules ($\text{CH}_2\text{Cl}_2/\text{CH}_3\text{CN}$, CH_3NO_2 , EtNO_2 , and dioxane) were obtained and analysed. In each case, the solvate structure displayed a similar centrosymmetric aromatic stacking complex in **1** with two included solvent molecules. These solvate crystals were all purple or purple-red in contrast with the orange colour of non-solvate crystal of **1**. This confirmed that the solvent molecules themselves were not participating directly in the CT complex

as the solvents varied widely in their atomic and electronic structures and yet all of the solvates of **1** had a similar purple colour. The only consistent difference between the solvate and non-solvate was in the orientation of the PYR and NDI surfaces as defined by the dihedral angle (θ) between the long axes of the two surfaces (Fig 4).³⁵ The purple solvate crystals consistently had θ angles greater than 50° (57° , 53° , $64\text{--}66^\circ$,³⁶ and 52°) and the orange non-solvate had θ values less than 50° (33 and 42°).³⁷ This same structural parameter (θ) has recently been identified by a recent computational study by Lin to help explain the orientations of PYR and NDI units in previous reported CT crystal structures.³⁸

The computational study by Lin predicted that θ angles from 50° to 75° would be the most thermodynamically stable for aromatic stacked PYR and NDI surfaces due to more favourable attractive electrostatic interactions.³⁸ This prediction is consistent with the observed geometries of the crystal structures of the **1** solvates. In the presence of included solvent, the PYR and NDI units of **1** have sufficient room and freedom to adopt the more stable stacking geometries ($\theta > 50^\circ$). The solvent molecules are able to fill the voids created by the more perpendicular X-shaped arrangement of the PYR and NDI units (Fig 1b). In contrast, in the absence of included solvent molecules, the PYR and NDI units adopt a more compact and aligned geometry ($\theta < 50^\circ$) to avoid forming voids. Thus the packing forces in the non-solvate structure prevent the PYR and NDI units from adopting the more stable X-shaped geometry.

In conclusion, we have developed an intramolecular CT molecule **1** which can reversibly change colour from purple to orange in the presence and absence of solvent in the solid-state. The colour switching abilities were attributed to solvent-induced changes in the intramolecular stacking geometry. The presence of solvent in the crystalline matrix allows the PYR and NDI units to form the more stable purple CT complex. In the absence of included solvent molecules, the PYR and NDI units are forced into a less stable orange CT complex. What is striking from the comparison of the crystal structures of **1** is how sensitive the CT band is to these subtle variations in the PYR-NDI dihedral angles. Small variations in θ angles ($\sim 10^\circ$) are readily observable by the naked-eye from the different colours of the resulting solids. Rathore and Kochi have previously shown that the intensity of the CT band and transition energies are highly sensitive to very small differences in the distances between aromatic donor and acceptor units.²¹ However, we have not come across a similar example demonstrating the sensitivity of the CT band to the orientations (angles) of the aromatic donor and acceptor units. This sensitivity could form the basis for a new type of intramolecular CT sensor, which can be read out by the naked-eye or inexpensive visible spectrometers. Further studies on the impact of the donor-acceptor orientation on the CT transition energy are currently underway in our laboratories.

This work was supported by SC EPSCoR GEAR:CRP grant. We are grateful to members of the zur Loye group for their help on the UV-vis spectroscopic measurements and images.

Notes and References

- ¹ G. Briegleb, *Elektronen-Donator-Acceptor-Komplexe*. Springer-Verlag, Berlin and New York, 1961.
- ² Z. X. Zhu, C. J. Cardin, Y. Gan, H. M. Colquhoun, *Nat. Chem.* 2010, **2**, 653.
- ³ H. M. Colquhoun, D. J. Williams, Z. Zhu, *J. Am. Chem. Soc.* 2002, **124**, 13346.
- ⁴ M. Kumar, K. V. Rao, S. J. George, *Phys. Chem. Chem. Phys.* 2014, **16**, 1300.
- ⁵ A. Das, S. Ghosh, *Angew. Chem., Int. Ed.* 2014, **53**, 2038.
- ⁶ K. Jalani, M. Kumar, S. J. George, *Chem. Comm.* 2013, **49**, 5174.
- ⁷ S. Burattini, B. W. Greenland, D. H. Merino, W. G. Weng, J. Seppala, H. M. Colquhoun, W. Hayes, M. E. Mackay, I. W. Hamley, S. J. Rowan, *J. Am. Chem. Soc.* 2010, **132**, 12051.
- ⁸ J. Fox, J. J. Wie, B. W. Greenland, S. Burattini, W. Hayes, H. M. Colquhoun, M. E. Mackay, S. J. Rowan, *J. Am. Chem. Soc.* 2012, **134**, 5362.
- ⁹ S. Burattini, H. M. Colquhoun, J. D. Fox, D. Friedmann, B. W. Greenland, P. J. F. Harris, W. Hayes, M. E. Mackay, S. J. Rowan, *Chem. Comm.* 2009, 6717.
- ¹⁰ T. Haino, A. Watanabe, T. Hirao, T. Ikeda, *Angew. Chem., Int. Ed.* 2012, **51**, 1473.
- ¹¹ (a) A. Das, S. Ghosh, *Angew. Chem., Int. Ed.* 2014, **53**, 1092; (b) A. Das, S. Ghosh, *Chem. Comm.* 2014, **50**, 11657.
- ¹² Y. K. Tian, Y. G. Shi, Z. S. Yang, F. Wang, *Angew. Chem., Int. Ed.* 2014, **53**, 6090.
- ¹³ A. S. Tayi, A. K. Shveyd, A. C. H. Sue, J. M. Szarko, B. S. Rolczynski, D. Cao, T. J. Kennedy, A. A. Sarjeant, C. L. Stern, W. F. Paxton, W. Wu, S. K. Dey, A. C. Fahrenbach, J. R. Guest, H. Mohseni, L. X. Chen, K. L. Wang, J. F. Stoddart, S. I. Stupp, *Nature* 2012, **488**, 485.
- ¹⁴ A. A. Sagade, K. V. Rao, U. Mogera, S. J. George, A. Datta, G. U. Kulkarni, *Adv. Mater.* 2013, **25**, 559.
- ¹⁵ P. Mukhopadhyay, Y. Iwashita, M. Shirakawa, S. Kawano, N. Fujita, S. Shinkai, *Angew. Chem., Int. Ed.* 2006, **45**, 1592.
- ¹⁶ R. D. Rasberry, M. D. Smith, K. D. Shimizu, *Org. Lett.* 2008, **10**, 2889.
- ¹⁷ D. R. Trivedi, Y. Fujiki, Y. Goto, N. Fujita, S. Shinkai, K. Sada, *Chem. Lett.* 2008, **37**, 550.
- ¹⁸ R. S. Mulliken, W. B. Person, *Annu. Rev. Phys. Chem.* 1962, **13**, 107.
- ¹⁹ (a) H. A. Staab, C. P. Herz, C. Krieger, M. Rentea, *Chem. Ber.* 1983, **116**, 3813; (b) H. A. Staab, G. H. Knaus, H. E. Henke, C. Krieger, *Chem. Ber.* 1983, **116**, 2785; (c) R. Reimann, H. A. Staab, *Angew. Chem., Int. Ed. Engl.* 1978, **17**, 374; (d) H. A. Staab, R. Reimannhaas, P. Ulrich, C. Krieger, *Chem. Ber.* 1983, **116**, 2808.; (e) H. A. Staab, G. Gabel, C. Krieger, *Chem. Ber.* 1983, **116**, 2827.
- ²⁰ L. G. Schroff, R. L. J. Zsom, A. J. A. Vanderweerd, P. I. Schrier, J. P. Geerts, N. M. M. Nibbering, J. W. Verhoeven, T. J. Deboer, *Recl. Trav. Chim. Pays-Bas* 1976, **95**, 89.
- ²¹ R. Rathore, S. V. Lindeman, J. K. Kochi, *J. Am. Chem. Soc.* 1997, **119**, 9393.
- ²² K. R. Leight, B. E. Esarey, A. E. Murray, J. J. Reczek, *Chem. Mater.* 2012, **24**, 3318.
- ²³ (a) B. K. Kaletas, R. Dobrawa, A. Sautter, F. Wurthner, M. Zimine, L. De Cola, R. M. Williams, *J. Phys. Chem. A* 2004, **108**, 1900.; (b) N. Van Anh, F. Schlosser, M. M. Groeneveld, I. H. M.; van Stokkum, F. Wurthner, R. M. Williams, *J. Phys. Chem. C* 2009, **113**, 18358.
- ²⁴ B. Wang, E. V. Anslyn, *Chemosensors principles, strategies, and applications*. In Wiley Series in Drug Discovery and Development; John Wiley & Sons: Hoboken, N.J., 2011
- ²⁵ For synthesis details see SI.
- ²⁶ Y. S. Chong, W. R. Carroll, W. G. Burns, M. D. Smith, K. D. Shimizu, *Chem.–Eur. J.* 2009, **15**, 9117.
- ²⁷ R. D. Rasberry, K. D. Shimizu, *Org. Biomol. Chem.* 2009, **7**, 3899.
- ²⁸ CT molecule **1** appears to be locked in the *anti*-conformation due to restricted rotation with the PYR groups on opposite sides of the NDI surface (See Ref. 27). The rotational barrier for these N-arylimide rotor was previously measured to be 27 kcal/mol (Ref. 26), which is too high for isomerization to the *syn*-conformer at the room temperature. Furthermore, heating *anti*-**1** in solution and the solid-state at the elevated temperature (80 °C) for 24 h showed no indications of the *syn*-conformer when monitored by ¹H NMR.
- ²⁹ Q. Jiang, H. Y. Zhang, M. Han, Z. J. Ding, Y. Liu, *Org. Lett.* 2010, **12**, 1728.
- ³⁰ H. A. Staab, D. Q. Zhang, C. Krieger, *Liebigs Ann-Recl.* 1997, 1551.
- ³¹ M. R. Molla, S. Ghosh, *Chem.–Eur. J.* 2012, **18**, 9860.
- ³² The post-TGA sample of the purple solvate was a low crystalline solid form and displayed a red coloration (Fig S4).
- ³³ Exposing the purple and orange solid samples of **1** to solvent vapours for 5 h showed no noticeable colour change.
- ³⁴ The similarity in colour between single crystals and precipitates were further confirmed quantitatively by diffuse reflectance UV-vis spectroscopy of the single crystals (Fig S5).
- ³⁵ The distances between the PYR and NDI units were also examined (See Table S1 in SI) but no correlation of these distances with the colour of the crystals was observed.
- ³⁶ Two crystallographically independent molecules were observed in the **1**•(EtNO₂)₂ crystal structure.
- ³⁷ The two θ angles are both for the same orange non-solvate crystal of **1**. The pyrene arms are disordered with two distinct populations leading to two separate θ angles.
- ³⁸ M. Y. Yeh, H. C. Lin, *Phys. Chem. Chem. Phys.* 2014, **16**, 24216.